Reliability Assessment for NanoEngineered Fatigue Crack Sensor

Seth S. Kessler, Carolyn Schmidt and Christopher T. Dunn

Metis Design Corporation

IWSHM-2017

ABSTRACT

The present research presents a novel approach for monitoring fatigue crack growth. The sensor itself is a sheet of Carbon Nanotube (CNT) sandwiched between a pair of electrically insulating layers. Any crack growth below the sensor would disrupt the CNT electrical network, therefore increasing the network resistance. Using orthogonal parallel pairs of electrodes, one would be able to not only measure extent of a crack, but also deduce the orientation based on relative changes seen by each pair; a flaw growing towards an electrode would have a small effect, while growing parallel to an electrode pair would offer a significant measured change. Analytical results are presented along with experimental data for calibrated simulated crack growth in addition to actual fatigue crack growth in aluminum specimens. The eventual goal for the program is to couple this sensor with RFID technology to provide a passive and connector-less assessment of fatigue crack growth.

INTRODUCTION

While more complex Structural Health Monitoring (SHM) methodologies have been demonstrated with various levels of success, great benefit could be realized by extremely simple "fuse-style" sensors. In its simplest embodiment, a fuse-style sensor could just be a single conductive trace with a binary response; either a crack has grown long enough to break electrical continuity or not. Multiple traces can be patterned to produce a pseudo-digital response. The present work investigates a continuum crack gauge fabricated using commercial carbon nanotube (CNT) sheets embedded into a conformal sensor comprising of film adhesive and electrode layers. The CNT form a network resistance that increases with crack growth.

Seth S. Kessler, Metis Design Corporation, 205 Portland St. Boston, MA 02114, USA
Carolyn Schmidt, Metis Design Corporation, 205 Portland St. Boston, MA 02114, USA
Christopher T. Dunn, Metis Design Corporation, 205 Portland St. Boston, MA 02114, USA

MODELING

Using Ansys 18.1, a finite element model of the CNT sensor with a crack was created changing electrode spacing, electrode width, sheet resistance, and crack length. The finite element model consisted of a minimum of 4096 eight node plane230 elements with voltage degrees of freedom. The finite element model analyzes half the geometry, with 0.5 V applied to nodes on the right-hand side of the model to form an electrode, and 0 V applied to some nodes of the left-hand side of the model as a symmetry boundary condition. The crack was modeled by removing some of these 0 V nodes. Figure 1 shows the finite element results and fit to the data.

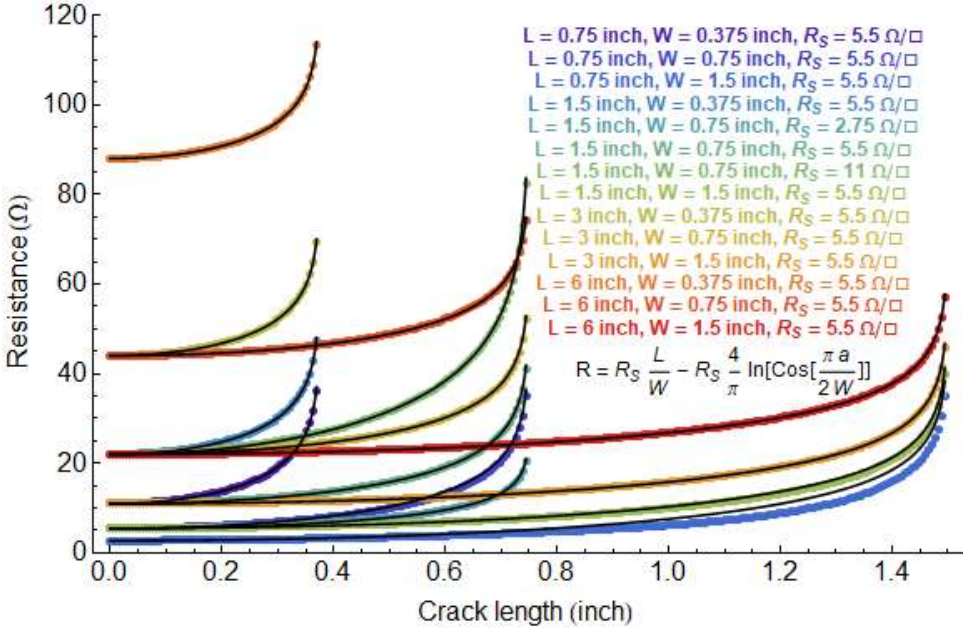

Figure 1. Finite element results plotting resistance versus crack length.

As can be seen in Figure 1, the resistance increases as a function of crack length. The finite element results in Figure 1 for the resistance, R, were fitted to:

$$R = R_0 - R_S \frac{4}{\pi} \ln\left(\cos\left(\frac{\pi\, a}{2\, W}\right)\right) \tag{1}$$

where R0 is the resistance of the sample without a crack:

$$R_0 = R_S \frac{L}{W} \tag{2}$$

These equations work well as a fit to the results, except for values of W / L of 2 or greater, that is a wide sample but a narrow electrode spacing. For small crack lengths comparted to the width Equation 1 is approximately given by:

$$R = R_0 + R_S \frac{\pi\, a^2}{2\, w^2} \qquad \text{small } a/w \tag{3}$$

PROOF OF CONCEPT

An experiment was devised to predict the extent and orientation of a growing flaw. The specimens were 15 cm square 7075 aluminum 1.5 mm thick plates to be representative of aircraft skin. First a 10 cm piece of adhesive film was placed in the center of each specimen. Next a 7.5 cm square piece of CNT sheet was placed over the film. Metal mesh was then placed in the center of each of the sides, 6 mm of overlap on CNT and 12 mm of overlap just on adhesive film. The width was picked used the previously described model as a good balance between sensitivity and coverage across the area based on the shape of the resulting electric field. A piece of surfacing film was placed over the CNT and overlapped mesh, and this entire assembly was vacuum bagged, debulked, and cured at 120˚C for 2 hours

Each specimen was loaded into a custom fixture to support it in a milling machine. A 0.5 mm carbide end mill was used to simulate crack growth in a specified orientation. First the end mill was plunged into the center of each specimen to create a 0.5 mm hole that was 1 mm deep, removed and data was collected. Next the end mill was returned to the hole and moved 0.5 mm at a time using the precision stage to extend the crack, while maintaining a 0.5 mm width and 1 mm depth. After each step the bit was retracted and data collected, and this process was repeated for a maximum flaw of 6 mm long. Two specimens were machined with cracks parallel to 2 sides, and two specimens were machined with a crack growing along the diagonal.

Figure 4 show the percentage change for each electrode pair versus crack length. Here the baseline resistance value is subtracted out before normalizing each data point with respect to change in resistance from the baseline condition. Each electrode pair is plotted along with a 2nd order polynomial fit. For the parallel crack growth specimens, there was virtually no change in the perpendicular direction and a very large change in the parallel direction. With the crack growing at a 45˚, the electrode pairs had nearly identical percentage changes in resistance, as expected. The datasets overlap at the 2nd point, as the initial hole looks the same to all electrodes.

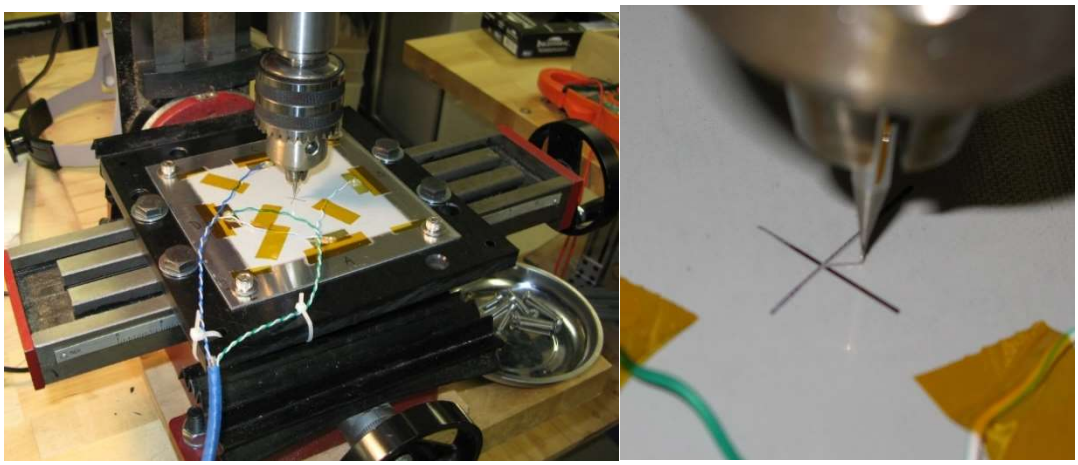

Figure 2. Various photographs of the experimental setup for calibrated flaw detection

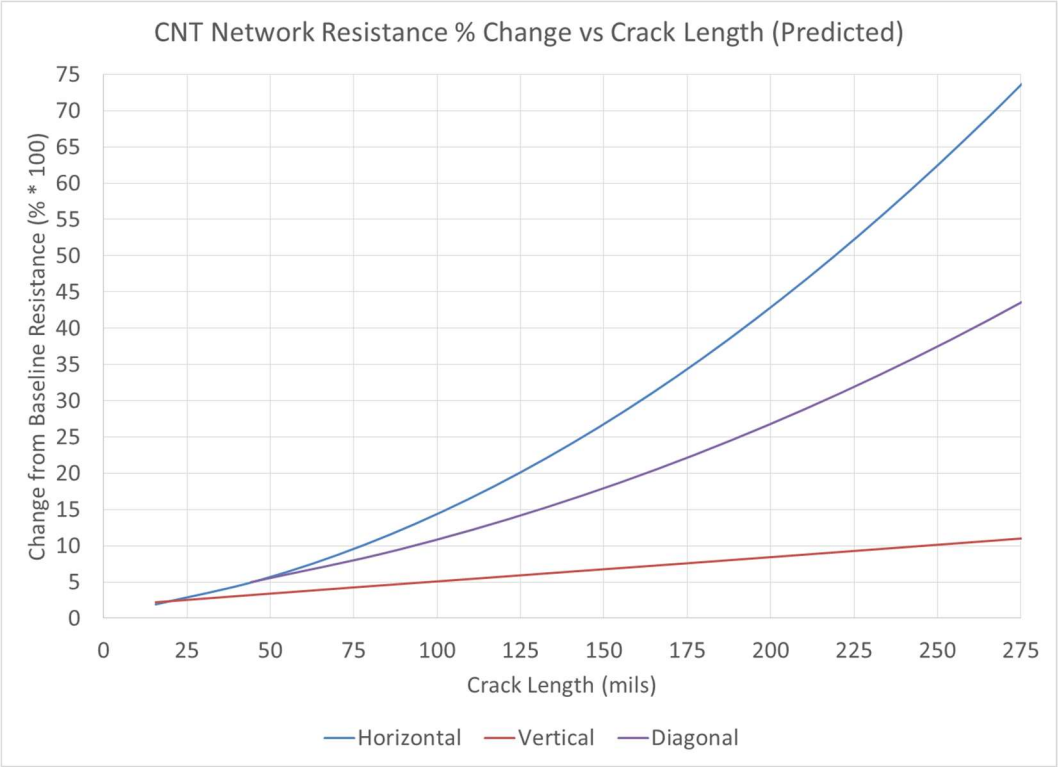

Figure 3. Predicted change in CNT patch resistance with crack length.

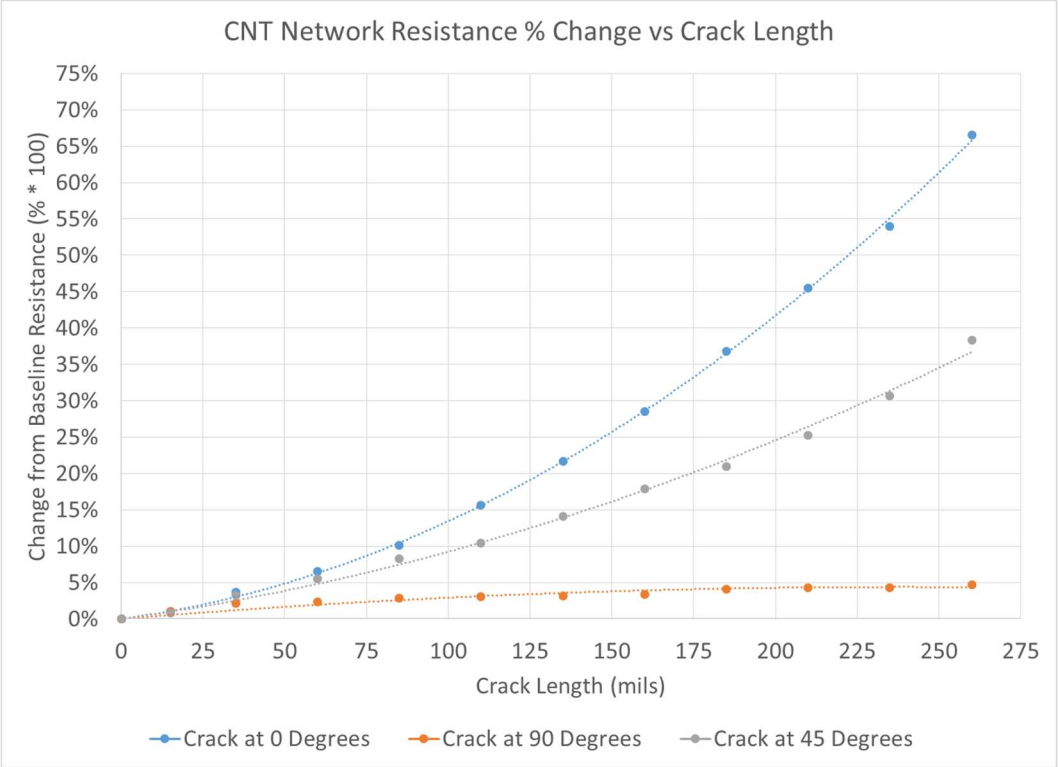

Figure 4: Percentage change plot for milled specimens, fit with 2nd order polynomials

EXPERIMENTAL SETUP

Each continuum crack gauge was built by sandwiching a sheet of CNT between layers of adhesive and electrically insulating films. The extremes of the CNT overlapped with an electrically conductive film that further contacted electrodes to monitor specimen resistance after each fatigue cycle. The sensor was a total of 150 micron thick with an active testing area of 5 x 2 cm. The cured CNT gauge was then bonded to a 6061-T6 Aluminum bar (30 x 2.5 x 0.3 cm) that had been wet sanded with 220 grit sandpaper and cleaned with isopropanol. Micro Measurements epoxy AE-10 was selected to bond the CNT gauge as it is commonly used for strain gauge installations. A notch was milled into each bonded coupon to initiate the fatigue crack. The notch was located in the center of the bar and extended 1.5 mm into the aluminum. The CNT region was set at 3 mm away from the bar's edge in order for the milled notch to end prior to the CNT.

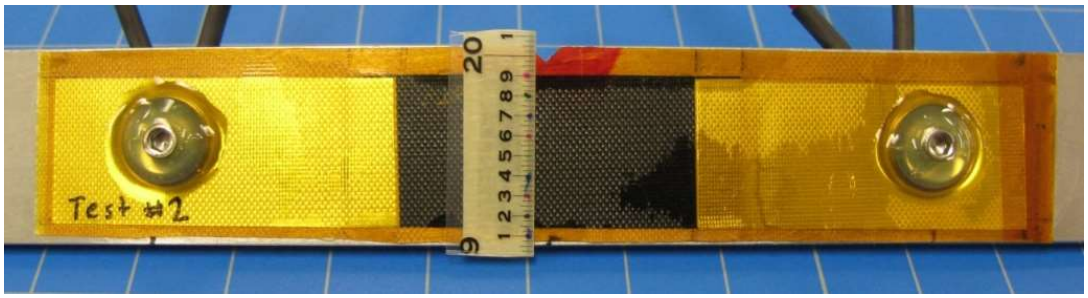

Figure 5. Various photographs of the experimental setup for calibrated flaw detection

A custom designed 4-point bend test rig was built to cycle each specimen using a precision stepper motor to propagate a fatigue crack. Each specimen was fatigued at 80% yield strain, achieved by a center roller displacement of 7.5 mm, for approximately 50,000 cycles to grow the crack at least 5 mm. The CNT gauge resistance was monitored after each fatigue cycle. During testing, an optical microscope (AmScope MU1000 series) was used to visually follow the crack. A Precision Clear Flexible Film Transparency Ruler by Ryan Precision Controls Products was attached to the crack gauge specimen to monitor crack growth and location. The ruler had minor tick marks 125 micron apart and major tick marks 625 micron apart. Different colored marks drawn on the ruler every 2.5 mm served as reference points to determine crack position along the specimen width. Crack length was monitored every 1,000 to 2,500 cycles during each test. An image of the crack was captured, followed by post-processing crack length measurements.

Figure 6: Photograph of 4-pt fatigue bend fixture (left) and fatigue crack growth (right)

EXPERIMENTAL RESULTS

Three preliminary specimens were fabricated and tested in the bend test rig as previously described. Each specimen represents a slightly varied configuration, namely a minor change in the external insulating layer. Table 1 summarizes the results of all three tests; specifically, the total number of cycles in the test, the number of cycles it took for the crack to propagate into the CNT region, the sample's initial resistance, and the sample's final resistance. Figure 7 illustrates the change in sensor resistance for each of the 3 configurations versus the optically measured fatigue crack length. It can be seen that all 3 configurations follow the model predictions quite well. Configuration 2 and 3 were more similar to each other (same material, just different surface treatments), which is reflected in how closely their resistance changes aligned. Specimen were cycled until yielding was apparent on their load-displacement curve, which is why the final crack length was different for each configuration. Figure 8 shows resistance versus cycles, illustrating the steady resistance value before cracking.

Table 1. Fatigue cycles for each specimen configuration with corresponding resistance values.

	Total Cycles	Cycles crack crossed CNT	Initial Resistance	Final Resistance
Configuration 1	43,000	16,000	17.65	26.86
Configuration 2	52,500	20,000	11.62	12.22
Configuration 3	45,000	12,500	10.50	11.50

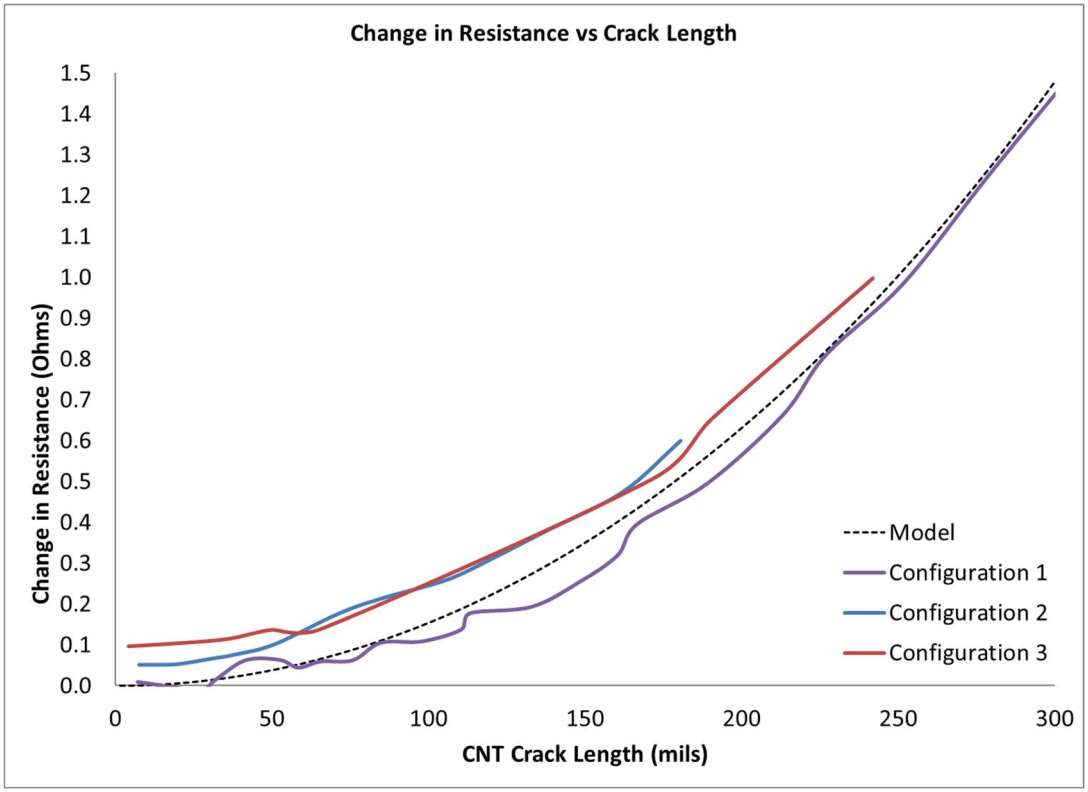

Figure 7. Experimental and predicted change in CNT sensor resistance with crack extension.

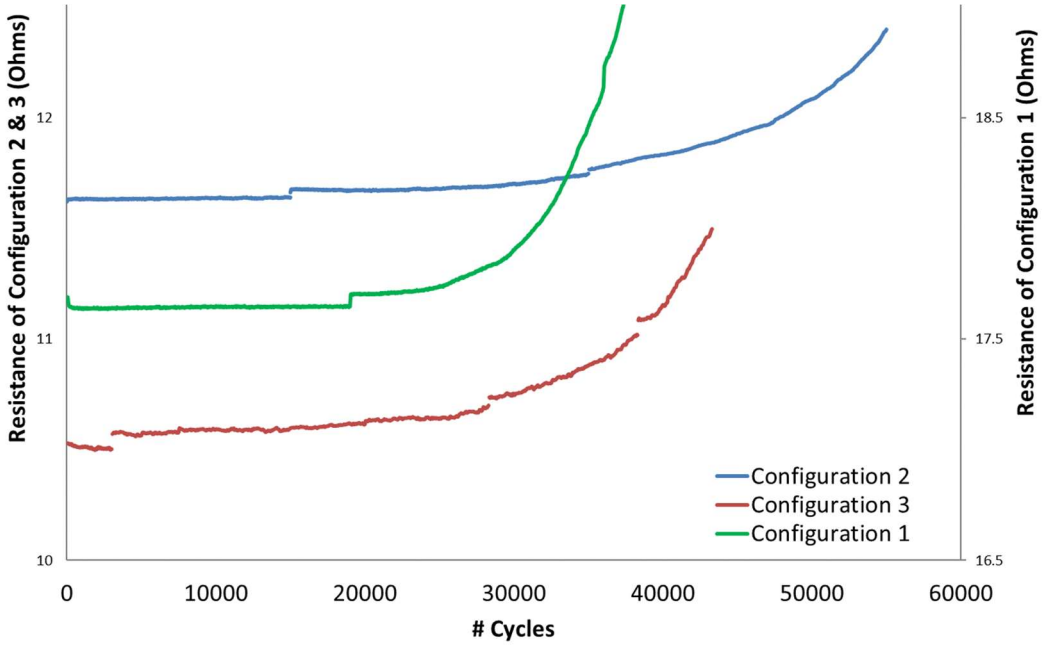

Figure 8. Experimental and predicted change in CNT sensor resistance with crack extension.

After testing, the CNT sensors were delaminated from their respective specimens to characterize the crack length in the aluminum specimens versus the crack length measured on the CNT crack gauge, mainly to witness if there were any significant shear-lag effects. The aluminum crack exhibited the meandering "zig-zag" crack evolution typical in fatigue specimens at a micro-scale, with the macro-scale crack growing in a relatively straight line across the specimen width. The corresponding CNT sensor crack was straighter, apparently "softening" the meandering effect, however the bulk crack formation remained largely the same as the crack in the aluminum. Table 2 compares both crack lengths, seen in Figure 9.

Table 2. Fatigue crack as measured on the specimen and the disbonded sensors.

	Al crack length (mm)	CNT crack length (mm)
Configuration 1	18	17
Configuration 2	7.0	6.0
Configuration 3	8.5	7.5

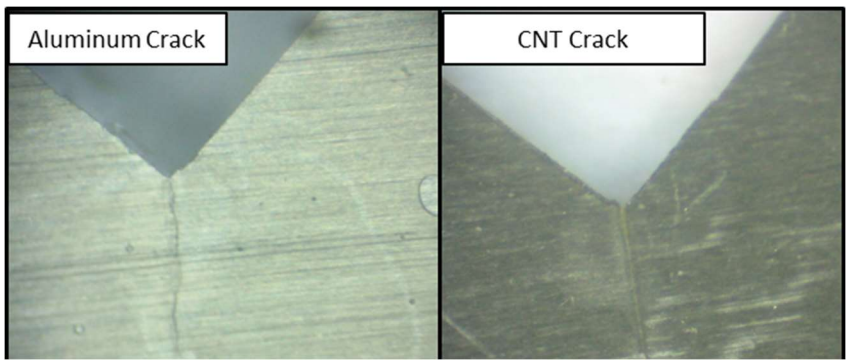

Figure 9: Photograph of corresponding cracks under microscope in aluminum (left) and CNT (right)

CONCLUSIONS

This paper presents a simple passive approach to monitoring fatigue cracks using CNT appliques. The applique is bonded to a structure similar to a strain gauge or conventional foil crack gauge, and the CNT sheet forms a network of resistors that increases as a crack grows across the sensor and increases the effective current path between electrodes. A simple FEM was built to predict this change in resistance versus crack length, and validated by milling a 0.5 mm channel on an aluminum plate. The final series of experiments present change in resistance for 3 configurations of the proposed CNT sensor that incorporate various electrically insulating layers. As can be seen in these results, the resistance changes for all 3 configurations were quite closely aligned, and well matched to the model prediction starting from around 0.25-0.5 mm crack length. The next stage of this research effort will include 6-12 repetitions of configuration 2 (most stable) in a controlled environment followed by tests at reduced and elevated temperatures and measurements under fixed strain values to produce a statistical model assisted probability of detection (MAPOD) curve according to MIL-HDBK-1823A. Finally, this CNT sensor will be coupled with RFID technology to provide a passive (RF power harvesting) wireless fatigue crack monitoring capability.

ACKNOWLEDGMENTS

This research was performed at the Metis Design Corporation in Boston, MA, and sponsored by the Air Force Research Laboratory under SBIR contract FA8650-14-M-2480.

REFERENCES

1. Raghavan A., Kessler S.S., Dunn C.T., Barber D., Wicks S. and B.L. Wardle. "Structural Health Monitoring using Carbon Nanotube (CNT) Enhanced Composites." Proceedings of the 7th International Workshop on Structural Health Monitoring, 9-11 September 2009, Stanford University.
2. Wicks S., Barber D., Raghavan A., Dunn C.T., Daniel L., Kessler S.S. and B.L. Wardle. "Health Monitoring or Carbon NanoTube (CNT) Hybrid Advanced Composite for Space Applications." Proceedings of the 11th European Conference on Spacecraft Structures, September 2009 Toulouse, France.
3. Barber D., Wicks S., Wardle B.L., Raghavan A., Dunn C.T. and S.S. Kessler. "Health Monitoring of CNT Enhanced Composites." Proceedings of the SAMPE Fall Technical Conference, October 2009, Wichita, KS.
4. Kessler S.S., Raghavan A., Dunn C.T., Wicks S., Guzman deVilloria R., and B.L. Wardle "Fabrication of a Multi-Physics Integral Structural Diagnostic System Utilizing Nano-Engineered Materials." Proceedings of the 2nd Annual Conference of the Prognostics and Health Management Society, October 2010, Portland, OR.
5. Wicks, S., Raghavan, A., Guzmán de Villoria, R., Kessler, S.S., and B.L. Wardle, "Tomographic Electrical Resistance-based Damage Sensing in Nano-Engineered Composite Structures," AIAA-2010-2871, *51st AIAA Structures, Structural Dynamics, and Materials (SDM) Conference*, Orlando, FL, April 12-15, 2010.
6. Guzman de Villoria, R., Kessler, S.S., Yamamoto, N., Miravete, A., and B.L. Wardle. "Multi-Physics Nano-engineered Structural Damage Detection and De-icing." Proceedings of the 18th International Conference on Composite Materials, 21-26 August 2011, South Korea.
7. Kessler S.S., Dunn C.T., Wicks S., Guzman deVilloria R.and B.L. Wardle. "Carbon Nanotube (CNT) Enhancements for Aerosurface State Awareness." Proceedings of the 8th International Workshop on Structural Health Monitoring, 12-15 September 2011, Stanford University.
8. Guzmán de Villoria, R., Yamamoto, N., Miravete, A., and B.L. Wardle, "Multi-Physics Damage Sensing in Nano-Engineered Structural Materials," online in *Nanotechnology*, April 2011.
9. Kessler S.S., Thomas G., Borgen M. and C.T. Dunn. "Performance Analysis for CNT-based SHM Composite Structures." Proceedings of the 9th Int'l Workshop on SHM, September 2013, Stanford University.
10. Kessler S.S., Thomas G., Borgen M. and C.T. Dunn. " Carbon Nanotube Appliques for Fatigue Crack Diagnostics." Proceedings of the 10th Int'l Workshop on SHM, September 2015, Stanford University.